Supporting Information

Low-Voltage, Long-Term Stable Organic Heterojunction Transistors with Broadband Bidirectional Photoresponse for In-Sensor Vision Computing

Yue Tian, Miao Cheng, Yifan Xie, Jinyao Wang, Changrui Liu, Jingyun Chu, Guoqing Xie, Neng Gao, Haofan He, Lejing Huang, Lingfei Wang, Panpan Zhang, Rongming Wang*, Mengmeng Li*

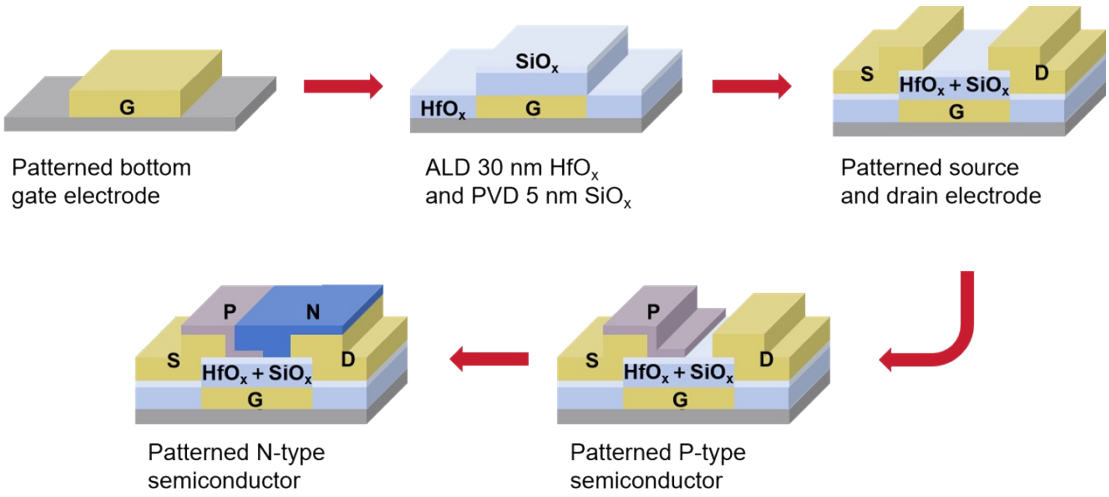

Figure S1. The preparation process of low-voltage organic sensors.

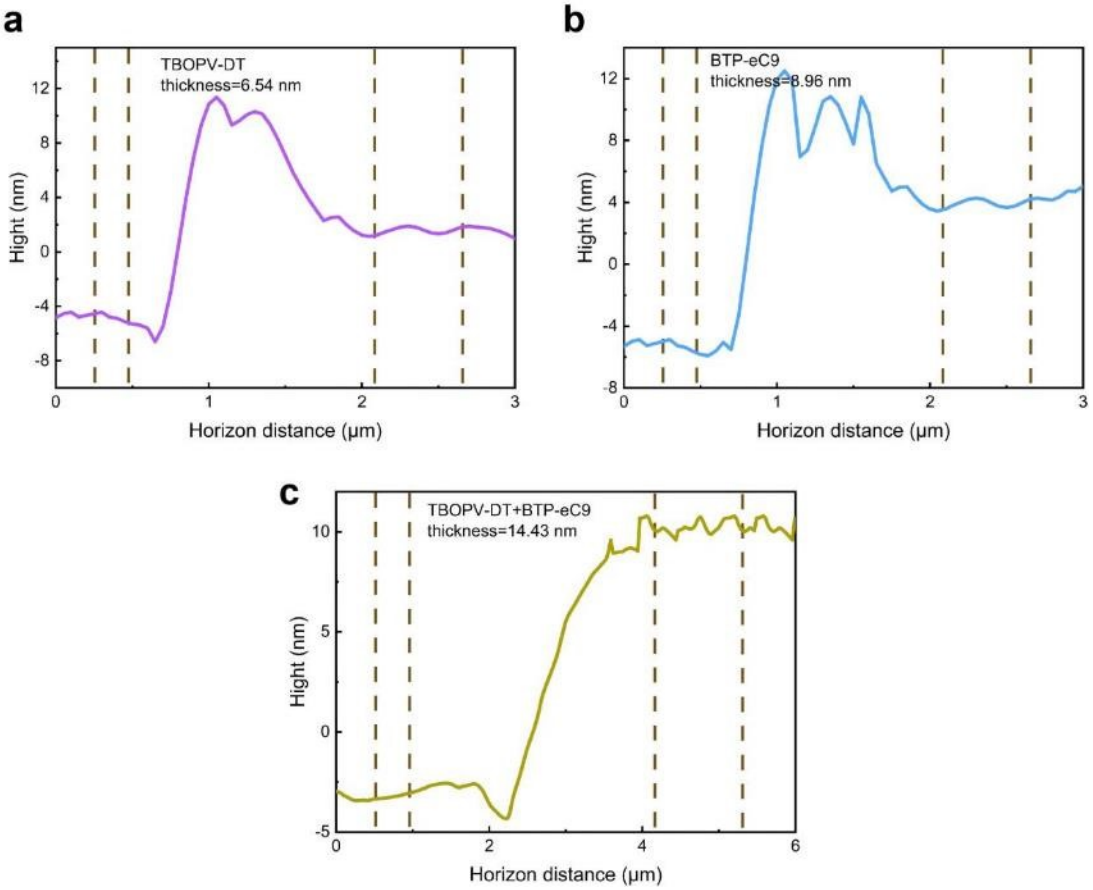

Figure S2. Thickness measurement of organic semiconductor films using AFM. (a,b) Single layer films of TBOPV-DT and BTP-eC9. (c) Bilayer films.

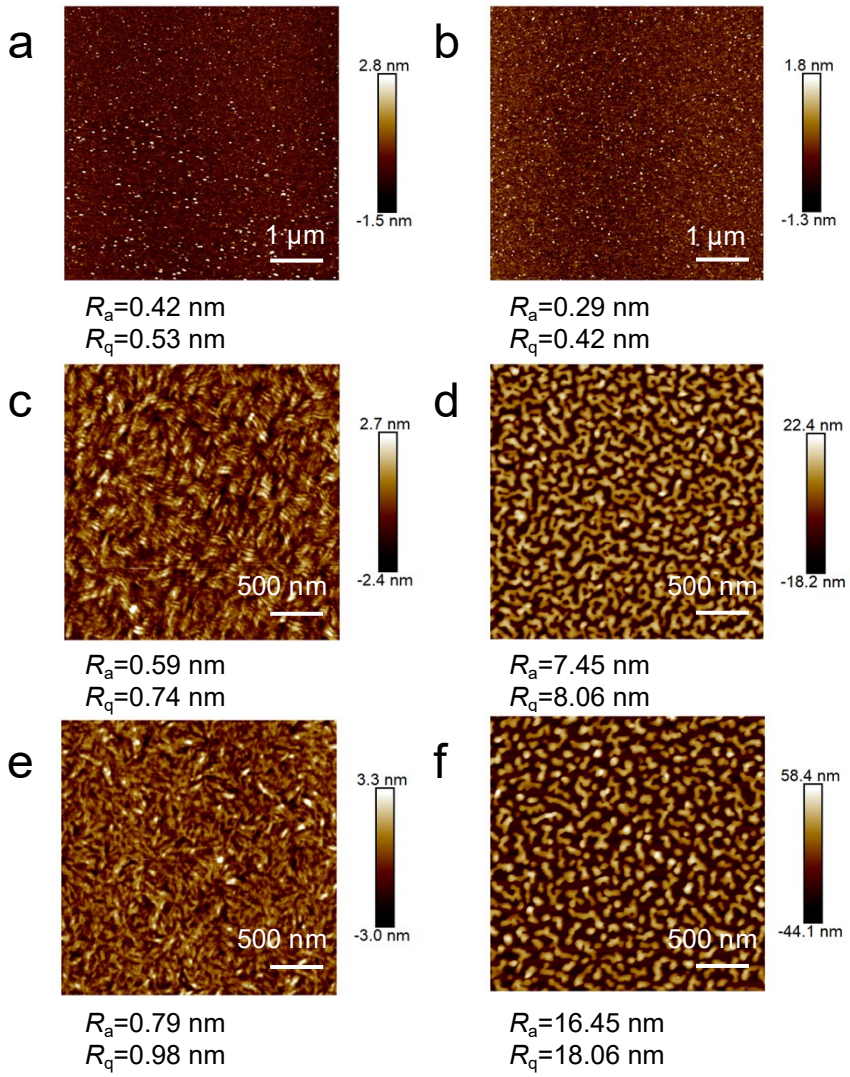

Figure S3. AFM images show the arithmetic mean roughness (R_a) and root mean square roughness (R_q) of the six surfaces (a) 30 nm HfO_2, (b) 30 nm HfO_2/5 nm SiO_2, (c, e) TBOPV-DT (P-type) on bare silicon oxide wafers and HfO_2 respectively, (d, f) BTP-eC9 (N-type) on bare silicon oxide wafers and HfO_2 respectively

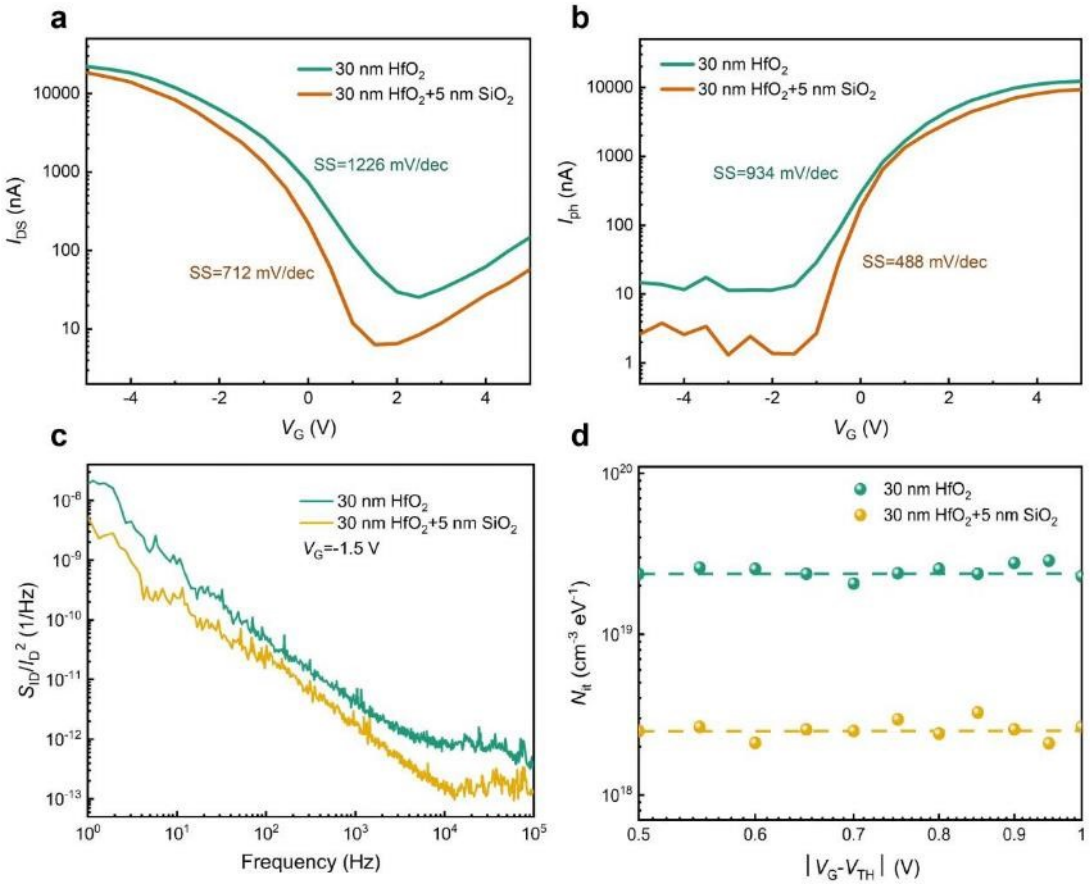

Figure S4. A comparative study on transfer characteristics curves of P-type (a) and N-type semiconductor (b) based on pristine HfO_2 and HfO_2 with SiO_2 composite dielectric layers. The SS value of pristine HfO_2 is larger. (c) The normalized noise current diagram of two types of dielectric layers. (d) Comparison of calculated N_{it} under different V_Gs.

The power spectral density of current noise, particularly the S_{ID} in field-effect transistors, can be described as[1]

$$S_{I_D} = g_m^2 \frac{e^2 kT\lambda N_{it}}{WLfC_{ox}^2} \quad [1]$$

where g_m, k, λ, N_{it}, f, and C_{ox} represent transconductance, Boltzmann constant, tunnel decay length, effective trap density, frequency, and gate capacitance, respectively. It is more convenient to use current-normalized S_{ID} as

$$\frac{S_{I_D}}{I_D^2} = \left(\frac{g_m}{I_D}\right)^2 \frac{e^2 kT\lambda N_{it}}{WLfC_{ox}^2} \quad [2]$$

Note that $\lambda = 0.2$ nm is used to estimate trap density (N_{it})[2].

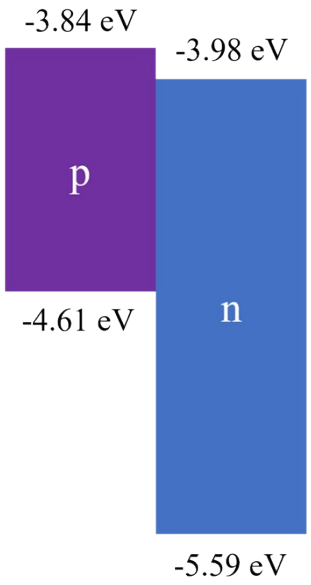

Figure S5. Energy band diagrams of organic semiconductors used in this study.

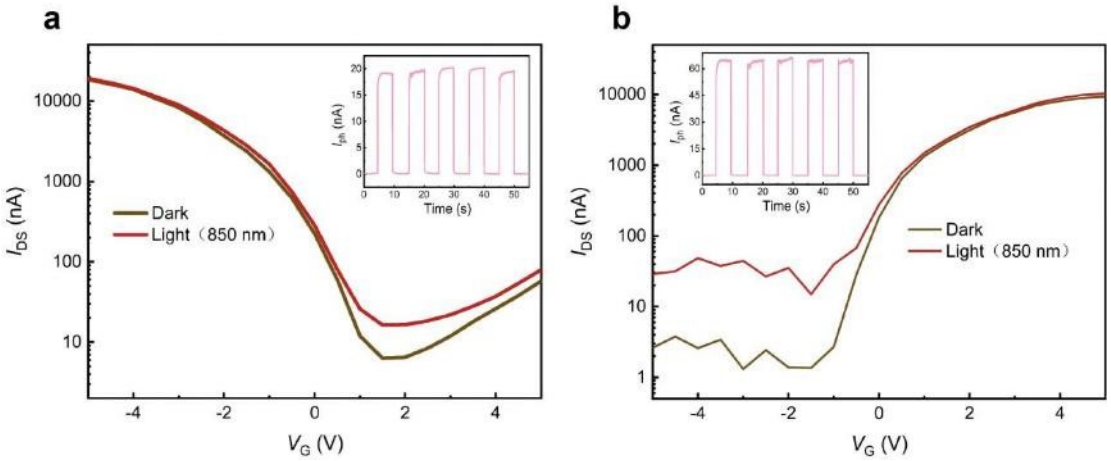

Figure S6. Transfer curves of the single-component OPTs. The organic semiconductors are (a) TBOPV-DT and (b) BTP-eC9, respectively. $|V_{DS}|$=5 V The inset shows the corresponding photocurrent-time plot with $|V_{DS}|$=5 V.

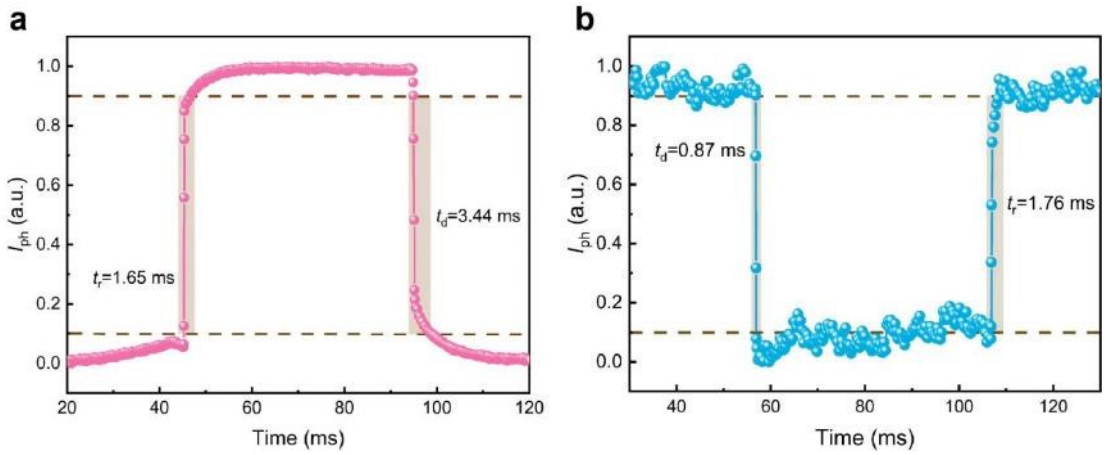

Figure S7. Analysis of the fast photoresponse characteristics under 850 nm illumination. Rise and decay times of the positive (a) and negative (b) photoresponses are defined as the time required for the net photocurrent to increase from 10% to 90% (or decrease from 90% to 10%) of its maximum value.

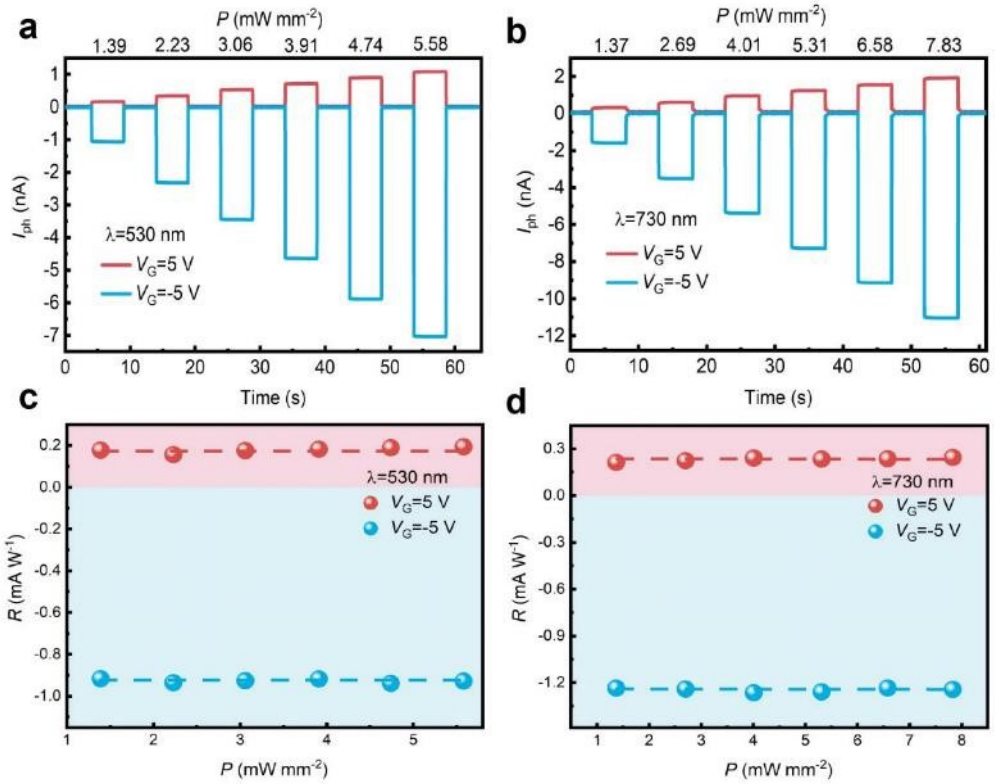

Figure S8. The positive and negative photocurrents of the device at ±5 V gate voltage under different illumination intensities at 530 nm (a, c) and 730 nm (b, d), along with the light-intensity-independent *R*s. V_{DS} = 5 V.

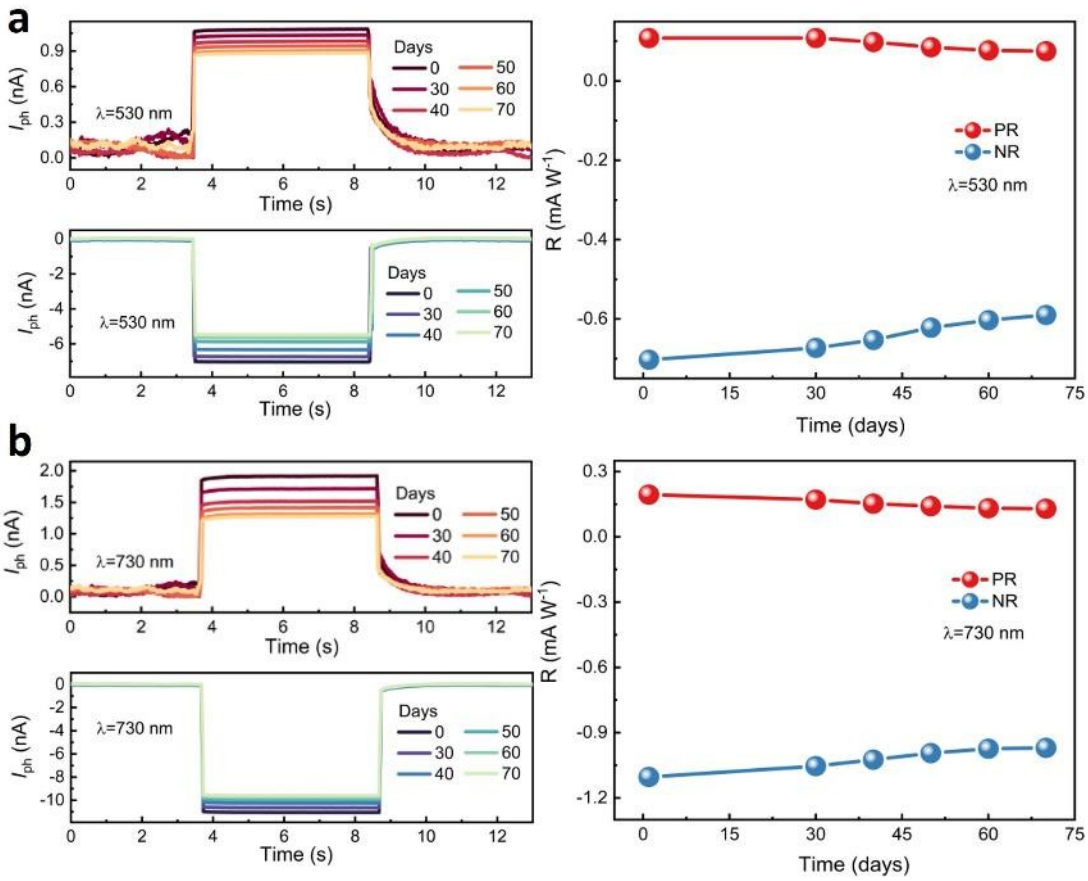

Figure S9. Over 70 consecutive days, I_{ph} and R variations were recorded every 10 days at the maximum intensity of 530 (a) and 730 nm (b) wavelengths. At 530 nm wavelength, the PR decreased by 20.5% while NR decreased by 25.4%. For 730 nm wavelength, PR showed a 17.7% decrease and NR experienced a 21.2% reduction.

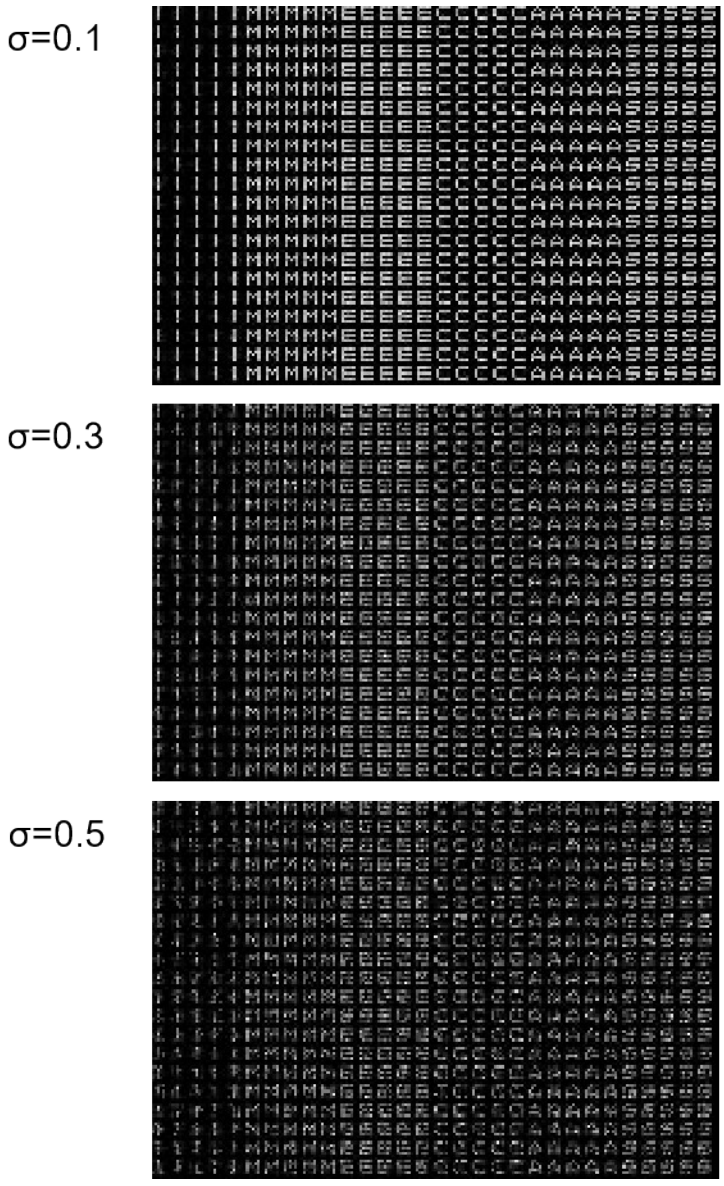

Figure S10. Training and testing dataset for letters classifier. The database is composed of six types of letters ("I" "M" "E" "C" "A" and "S") with 5×5 pixels. The total dataset has 1800 images with 300 images for each letter. Gaussian noise with different level (σ = 0.1, σ = 0.3, and σ = 0.5) has been add to the images.

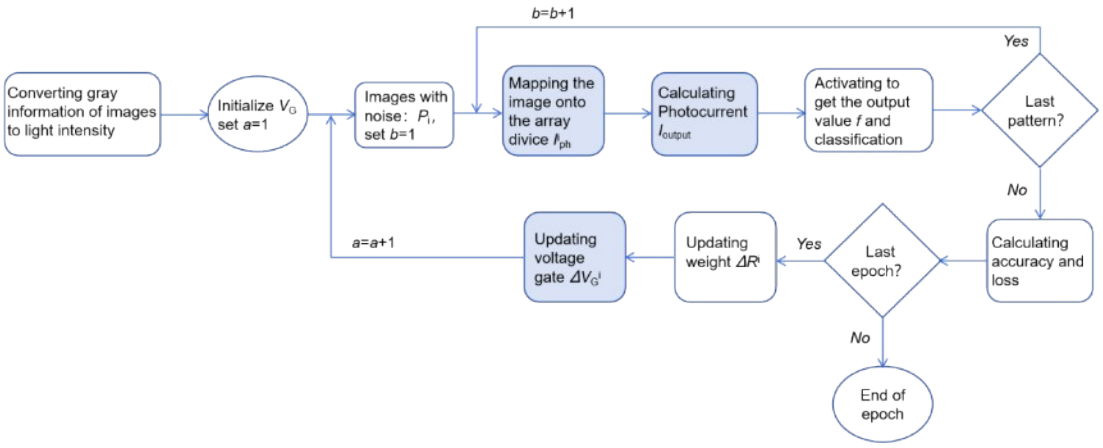

Figure S11. Flow chart of the training algorithm of the letter classifier. The shaded boxes are fulfilled by the in-sensor computing device array, and the white processing boxes are simulated using software.

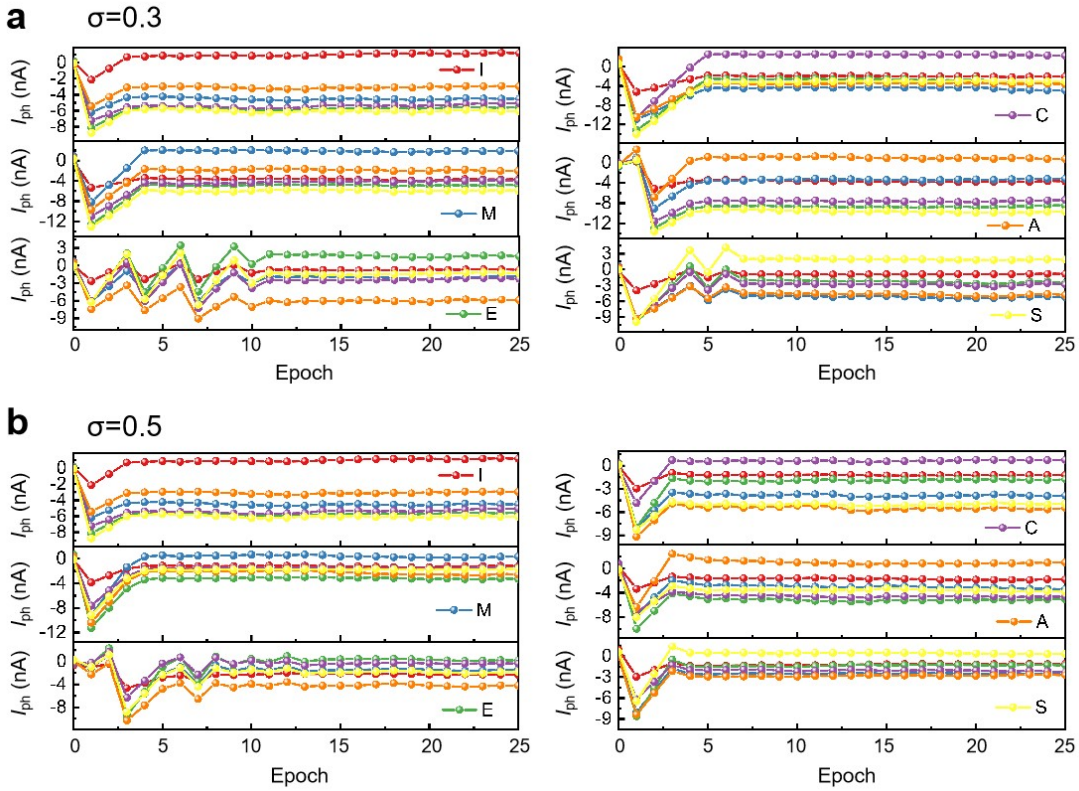

Figure S12. The changing process of output photocurrent of different neurons at the Gaussian noise level of σ = 0.3 (a) and σ = 0.5 (b). As the number of training epoch increases, the output current presents a positive and negative bipolar distribution. The highest output value represents the classify result of the neuron, and the target letters can be well separated after 3-4 epochs.

Table S1. Summary of device performance for organic semiconductor based phototransistors.

Semiconductor	λ (nm)	opt. volt (V)	Response characteristics	R (mA/W)	t_r/t_d (ms)	Ref.
DPA	430	-100~20	PR	1.34×10^8	-	3
TDPPQ	360-940	-20~60	PR	9.2×10^8	-	4
BODIPY-BF2	460~940	-5~40	PR	1.14×10^7	2.98/4.95	5
DPP-DTT	850	-30~30	PR	246000	3600/4200	6
P3HT/PDPPTTT	450~795	-40~40	PR	＜1000	-	7
TIPS−PEN/CuPc	460~620	-30~0	PR	50	600/600	8
CuPc/p-6P	365	-40~40	PR	2.2×10^7	＞100	9
VOPc/p-6P	365	-40~40	PR	1.5×10^8	-	10
C60/AlClPc	450	-50~80	PR	94400	0.244/0.548	11
P3HT/THBT-ht	470~665	-80~20	PR	4000	-	12
p-7P/F16CuPc	365	-50~50	PR and NR	85300	-	13
TBOPV-DT/BTP-eC9	**530~1050**	**-5~5**	**PR and NR**	**0.23**	**1.65/3.44 for PR; 1.76/0.87 for NR**	**This work**

References

[1] S. Watanabe, H. Sugawara, R. Häusermann, B. Blülle, A. Yamamura, T. Okamoto and J. Takeya, *Communications Physics*, 2018, **1**, 37.

[2] P. Srinivasan, E. Simoen, L. Pantisano, C. Claeys and D. Mirsa, *Microelectron Eng*, 2005, **80**, 226-229.

[3] D. Ji, T. Li, J. Liu, S. Amirjalayer, M. Zhong, Z.-Y. Zhang, X. Huang, Z. Wei, H. Dong, W. Hu and H. Fuchs, *Nature Communications*, 2019, **10**, 12.

[4] Y.-S. Guan, J. Qiao, Y. Liang, H. K. Bisoyi, C. Wang, W. Xu, D. Zhu and Q. Li, *Light: Science & Applications*, 2022, **11**, 236.

[5] F. Li, Y. Chen, C. Ma, U. Buttner, K. Leo and T. Wu, *Advanced Electronic Materials*, 2017, **3**, 1600430.

[6] Y. Lei, N. Li, W.-K. E. Chan, B. S. Ong and F. Zhu, *Organic Electronics*, 2017, **48**, 12-18.

[7] S. Nam, H. Han, J. Seo, M. Song, H. Kim, T. D. Anthopoulos, I. McCulloch, D. D. C. Bradley and Y. Kim, *Advanced Electronic Materials*, 2016, **2**, 1600264.

[8] A. K. Mahato, V. Raghuwanshi, D. Bharti, I. Varun, N. Prasad, M. S. Roy and S. P. Tiwari, *Synthetic Metals*, 2019, **248**, 110-119.

[9] C. Qian, J. Sun, L.-A. Kong, G. Gou, M. Zhu, Y. Yuan, H. Huang, Y. Gao and J. Yang, *Advanced Functional Materials*, 2017, **27**, 1604933.

[10] C. Qian, J. Sun, L.-a. Kong, Y. Fu, Y. Chen, J. Wang, S. Wang, H. Xie, H. Huang, J. Yang and Y. Gao, *ACS Photonics*, 2017, **4**, 2573-2579.

[11] L. Du, X. Luo, F. Zhao, W. Lv, J. Zhang, Y. Peng, Y. Tang and Y. Wang, *Carbon*, 2016, **96**, 685-694.

[12] H. Han, S. Nam, J. Seo, J. Jeong, H. Kim, D. D. C. Bradley and Y. Kim, *IEEE Journal of Selected Topics in Quantum Electronics*, 2016, **22**, 147-153.

[13] D. Xue, W. Gong, C. Yan, Y. Zhang, J. Lu, Y. Yin, J. Zhang, Z. Wang, L. Huang and L. Chi, *Advanced Functional Materials*, 2024, **34**, 2402884.